



Published in final edited form as:

Nat Neurosci. ; 15(7): 949–951. doi:10.1038/nn.3134.

Pattern, and not magnitude, of neural activity determines dendritic spine stability in awake mice

Ryan M. Wyatt*, Elaine Tring*, and Joshua T. Trachtenberg

Department of Neurobiology David Geffen School of Medicine at UCLA

Abstract

The stability of dendritic spines in the neocortex is profoundly influenced by sensory experience, which determines the magnitude and pattern of neural firing. By optically manipulating the temporal structure of neural activity *in vivo* using channelrhodopsin-2 and repeatedly imaging dendritic spines along these stimulated neurons over weeks, we show that the specific pattern, rather than the total amount of activity, determines spine stability in awake mice.

Synaptic connections in mammalian cortex are strongly modified by experience, injury, and learning¹. Changes in neural connectivity in the cortex, culminating in the growth and retraction of synapses, contribute to changes in neural function. Because of the profound effects that experience has upon synaptic connectivity, the role of neural activity in regulating synaptic stability has been intensively studied. This question has recently been addressed in primary sensory cortices using *in vivo* vital imaging techniques to demonstrate that sensory deprivation is able to regulate the fates of dendritic spines²⁻⁴, the postsynaptic components of excitatory synapses. Whether changes in dendritic spine stability are influenced by changes in total neural activity or by changes in the pattern of this activity is not known.

To investigate the relative influence of total firing versus firing pattern on spine stability in neocortex we chronically stimulated layer 5 (L5) pyramidal neurons in awake, behaving mice 8 hours per day for a period of 7 days and repeatedly imaged dendritic spines from a subset of these cells using chronic *in vivo* 2-photon imaging techniques. To achieve this, we bred mice expressing YFP-tagged channelrhodopsin-2 in neocortical L5 pyramidal neurons with mice expressing a cytosolic GFP that labels a subset of L5 pyramidal neurons in their entirety. That neurons expressing GFP also expressed ChR2 was confirmed using laser capture quantitative rtPCR (**Supplementary Fig. 1**).

To select a chronic stimulation protocol, we wanted to utilize physiologically relevant frequencies that approximated average firing patterns of somatosensory cortical L5 cells in

Users may view, print, copy, download and text and data- mine the content in such documents, for the purposes of academic research, subject always to the full Conditions of use: http://www.nature.com/authors/editorial_policies/license.html#terms

*These authors contributed equally to this work

Author Contributions

R.W. conducted the longitudinal dendritic spine imaging experiments, analyzed the data and wrote the manuscript. E.T. conducted the awake, behaving cell attached patch recordings. J.T. designed and supervised the project and wrote the manuscript.

recruitment of FS interneurons, as shown above, which would suppress extraneous spiking. In contrast, spontaneous activity during 2 Hz bursts was not significantly different than during periods of no stimulation (**Fig. 1c**, $P = 0.75$). When we counted the total number of spikes that occurred during 10-second epochs (inclusive of evoked and spontaneous activity) when cells were either stimulated with 2 Hz bursts every 2 seconds ($n=29$ epochs) or 10 Hz bursts every 10 seconds ($n=29$ epochs), we found no significant difference in the distributions between the two groups (**Fig. 1d**, $P = 0.18$). Thus, the total amount of activity was held constant between the two groups while the evoked firing frequency differed by a factor of 8 in awake, behaving mice.

To examine how these different firing patterns impacted spine stability, we used 2-photon excitation to image the fine structure of the apical dendrites of GFP-expressing L5 pyramidal neurons in somatosensory cortex *in vivo*. Dendrites and dendritic spines were first imaged on postnatal day 28 (P28), one day prior to the onset of optical stimulation, and at P36, one day after the end of the week-long stimulation trial (**Fig. 2a**), and a third time at P43, one week after the termination of optical stimulation. The same dendritic domains were imaged on all three time points and the fates of dendritic spines were tracked (Control: $n=3$ mice, 6 cells, 19 dendritic branches, 737 spines; 2 Hz: $n=4$ mice, 7 cells, 21 branches, 696 spines; 10 Hz: $n=6$ mice, 8 cells, 24 branches, 749 spines). Repeated optical stimulation with 10 Hz trains for seven days resulted in an approximately 25% reduction in the percentage of eliminated spines compared to unstimulated or 2 Hz stimulated mice. In contrast, 2 Hz trains did not significantly impact rates of spine elimination compared to controls (**Fig. 2b**; unstimulated control: $24.5 \pm 1.8\%$ loss, 10 Hz stimulated: $18.0 \pm 1.1\%$, 2 Hz stimulated: $22.5 \pm 1.6\%$; ANOVA: $P < 0.01$; post hoc test: 10 Hz versus control, $P = 0.005$; 2 Hz versus control, $P = 0.66$). Measures of the relative size of eliminated spines - a measure of synaptic strength⁸ - showed no differences across groups (**Fig. 2c**), indicating that our stimulation paradigm was not causing the loss of a specific sub-group of spines. In addition to reduced spine elimination, we also found an approximately 30% reduction in the percentage of new spines formed in the 10 Hz stimulated mice compared to unstimulated controls. 2 Hz stimulation did not appreciably alter fractional spine gain (**Fig. 2b**; unstimulated control: $15.3 \pm 1.5\%$ gain, 10 Hz stimulated: $10.5 \pm 1.3\%$, 2 Hz stimulated: $14.2 \pm 1.3\%$; ANOVA: $P < 0.05$; post hoc test: 10 Hz versus control, $P = 0.03$; 2 Hz versus control, $P = 0.81$).

Spine density in unstimulated mice decreased by 11% between P28 and P36 (0.45 ± 0.03 spines/ μm at P28, 0.40 ± 0.02 spines/ μm at P36; $P < 0.01$). Similar reductions in spine densities were observed in both the 10 Hz stimulated (~8% decrease; 0.51 ± 0.02 spines/ μm at P28, 0.47 ± 0.02 spines/ μm at P36; $P < 0.01$) and 2 Hz stimulated groups (~9% decrease; 0.48 ± 0.02 spines/ μm at P28, 0.44 ± 0.02 spines/ μm at P36; $P < 0.001$). While the reduction in spine density was somewhat greater in the control mice than either stimulated group, this difference was not statistically significant (**Fig. 2d**, ANOVA: $P = 0.54$). These results indicate that while the magnitude of spine growth and retraction is regulated by the pattern of activity, spine density is not.

To examine whether the observed effects on synaptic stability were permanent or whether they depended on continual stimulation, we stopped delivering optical stimuli after the first week (P36) and then re-imaged the same dendrites one week later at P43 (**Fig. 2a**). We

found no significant differences in fractional spine gain or loss between any of the groups over this week (**Fig. 2e**; Elimination, ANOVA $P = 0.56$; Gain, ANOVA $P = 0.34$). Accordingly, there were no significant differences in overall spine density (unstimulated, 0.39 ± 0.02 spines/ μm ; 10 Hz, 0.45 ± 0.02 spines/ μm ; 2 Hz, 0.42 ± 0.02 spines/ μm ; ANOVA, $P = 0.11$).

Sensory experience alters the pattern of neural activity more so than firing rate^{9, 10}, and learning enhances temporal correlations in neural ensembles in cortex¹¹. Our results show that the pattern of neural activity, and not the absolute number of spikes fired, determines the stability of dendritic spines and, by extension, excitatory synapses in the cortex. Comparable experiments in the developing neuromuscular junction yielded similar conclusions¹². Taken together, these results support a view in which firing pattern is the major conveyor of information in the nervous system, a view that has gained recent support by investigations of axon segregation in the developing colliculus¹³. Our findings leave open a number of explanations for the source of increased spine stability. One possibility, which we favor, is that the firing pattern of the parent neuron, rather than the pattern of global network activity, drives spine stability. Alternatively, spiking of L5 neurons may recruit local GABAergic circuitry in L1, the layer in which the dendrites we imaged reside. Local dendritic inhibition may influence spine stability more strongly than the intrinsic activity of the L5 neuron. FS interneurons, which preferentially innervate excitatory cell somas, are strongly recruited by optical stimulation of L5 neurons (cf. **Fig. 1a**). Less clear is whether somatostatin-expressing interneurons, which innervate the apical dendrites imaged here and would therefore be the likely source of dendritic inhibition¹⁴, are also recruited by L5 activity. In either scenario it is the pattern, not the magnitude of activity is what matters most. The importance of firing pattern on synaptic stability is perhaps most elegantly demonstrated in song birds where juveniles learn to sing by matching their own song to a memorized tutor song. During the period of exposure to a specific pattern of instructive experience (the tutor song) dendritic spines are rapidly stabilized¹⁵ - an effect that is mirrored in our experiments by 10 Hz bursts.

ONLINE METHODS

All experimental procedures were approved by the University of California Los Angeles Office of Animal Research Oversight and the Chancellor's Animal Research Committee.

Subjects

Mice expressing the channelrhodopsin-2 transgene driven by the *thy1* promoter¹⁶ (line 18) were purchased from Jackson Laboratories (Stock #007612) and also generously given to us by G. Feng. These mice were bred with *Thy1-GFP* mice¹⁷ (M line). Offspring from these crossings were used for our experiments. GFP expression was confirmed visually by examining ear clippings under a fluorescence microscope. ChR2 expression was confirmed via PCR using the following primers: TCT GAG TGG CAA AGG ACC TTA GG (forward); GAA GAT GAC CTT GAC GTA TCC G (reverse).

Laser capture microdissection (LCM)

was performed on brains from 4 double transgenic mice (*Thy1-ChR2-YFP* x *Thy1-GFP*) and 2 wild type mice. Briefly, brains were dissected, frozen on dry ice, and sectioned at 10 μ m. Sections taken from somatosensory cortex were placed on uncoated glass slides followed by dehydration in 80% (1 min), 90% (30 sec), 2x 100% ethanol (30 sec) followed by two rinses in xylene. Slides were air-dried and immediately submitted to LCM. eGFP positive cells from layer 5 were laser captured (Veritas System, Molecular Devices) with the following parameters: spot size 11 μ m, pulse duration 1.5 msec, power 55–60 mW. 15 to 20 neurons were captured from layer 5 of both cortical hemispheres in each section through somatosensory cortex, for a total of 300 cells from each group. To avoid RNA degradation, cells were captured within 60 minutes for each cap and transferred to the RNA lysis buffer. Total RNA was extracted from isolated cells with the Mini RNA isolation kit (Zymo Research), according to the manufacturer's protocol. Isolated RNA was subjected to two rounds of T7 amplification (TargetAmp, Epicenter). After the second round of cDNA synthesis, samples were examined by real-time qPCR as described for the expression of GAPDH, GFP and ChR2. Values are expressed as the concentration ratio of gene expression normalized to GAPDH.

Recordings of spontaneous activity in awake mice on a running ball

We followed the protocol outlined in reference (18). To habituate mice to head restraint, mice were handled on the first day of training by repeatedly picking them up. On the second day, a metal bar later used to restrain the animal was epoxied to the mouse's skull. On the third day, mice were placed on a floating Styrofoam ball, head fixed and allowed to run for two 10 minute sessions with a 10 minute break in between. This was repeated daily for 3 days. On the day of recording a small burr-hole was made directly over somatosensory cortex. Loose cell-attached patch recordings were made from 18 layer 5 neurons. Laminar position was based on depth. Contact of the pipette tip with the cell was judged by the concurrence of a sudden increase in resistance and proximity of pipette tip to the soma. Pressure was released, to 0 mbar. Spike waveforms were used to distinguish between regular-spiking and fast-spiking cells¹⁹. Electrode resistances were between 3-5 M Ω . Seals of 0.03 – 1 G Ω resistance were found to be sufficient to detect and isolate the spikes of single neurons. Five minute recordings were made from each cell. Electrophysiological signal was acquired with a Multiclamp amplifier in current-clamp mode, National Instruments digitizer, and WinEDR software (J Dempster, Strathclyde University). Data were analyzed in Matlab and Clampfit. Signal was sampled at 10 kHz and filtered at 6 kHz. Pipette capacitance was compensated. Solutions were as follows, internal (in mM): 105 K-gluconate, 30 KCl, 10 HEPES, 10 phosphocreatine, 4 ATP-mg, 0.3 GTP. Cortex buffer (in mM): 125 NaCl, 5 KCl, 10 glucose, 10 HEPES, 2 CaCl₂, 2 MgSO₄.

Recordings of light-evoked activity in awake mice on a running ball

Mice were habituated as above. Instead of a burr hole, a 2mm craniotomy was made and a coverslip was placed over the craniotomy, leaving a 1mm gap for recording access. Additionally, pipettes were filled with cortex buffer. For each recorded cell, 5-minute runs were recorded with 10 Hz light trains, and, subsequently, 5-minute runs were recorded with

2 Hz light trains. Recordings were made blind. Fast spiking interneurons were identified using wave-form analysis as detailed in reference (19). Spikes were classified as light-evoked if they were time-locked with either the onset of the LED stimulus (FS interneurons) or the offset (L5 excitatory neurons fired as the local field potential was decaying). All spikes not time locked to the stimulus during the 1-second light stimulation period were classified as 'spontaneous'.

Cranial window surgery

Cranial windows were prepared as in reference (20). To optically stimulate through the cranial window, a blue high powered LED (Nichia Corporation; NFSB036BT-E) was fixed to a removable head cap that could be secured directly over the cranial window. The pattern of light stimulation was controlled using a Master-8 stimulator (AMPI; Jerusalem, Israel). Each pulse to the LED was 3.8 V and 10 ms in duration. Highly flexible earphone wire was used to connect the stimulator to the head-fixed diode on the mouse. Mice were stimulated for 8 hours each day for 7 days in the light, were able to freely move around their cage, and had free access to food and water. At the end of each 8 hour stimulation period, the LED head caps were removed, the mice were placed back in their home cage and were returned to the vivarium.

Cortical temperature

was measured during a 1-hour exposure 10 Hz blue light trains with the LED-head cap secured directly over the cortex as during awake stimulation experiments. We used a HYPO-33-1-T-G-60-SMP-M thermocouple from Omega.com, with a needle diameter of 0.2mm. Temperature measures were made every 10 seconds. Brain temperature fluctuated over a 0.3 degree temperature range over the course of the hour.

Longitudinal *in vivo* 2-photon imaging

GFP-labeled neurons in the somatosensory cortex were imaged *in vivo* using a custom-built 2-photon laser scanning microscope using ScanImage acquisition software written in MatLab²¹. GFP was excited at 910nm. Emitted photons were filtered with a Semrock FF01-514/30 bandpass filter and a Semrock FF01-750/SP laser blocking emission filter. Filtered photons were detected with a Hamamatsu R3896 photomultiplier tube. Analysis of spines was performed using ScanImage software following the guidelines established in reference (20). The percentage of gained or eliminated spines was calculated as the number of spines added or lost between two time points, respectively, divided by the total number of preexisting spines. Relative spine size, a measure that includes both the number of pixels and the pixel intensity of each spine, was calculated as in reference (22). Briefly, the background subtracted summed pixel value of a spine was divided by the average background subtracted pixel intensity of a nearby segment of dendritic shaft to correct for inhomogeneities in fluorescence excitation. In this measure, the resultant units are in pixels and reflect the normalized size of the spine. Spine turnover and density data is presented as mean \pm s.e.m. P values across the 3 experimental groups were obtained via a one-way ANOVA. Tukey-Kramer multiple comparison post-hoc tests were performed to compare means between individual groups.

Supplementary Material

Refer to Web version on PubMed Central for supplementary material.

Acknowledgements

We wish to thank S. Thomas Carmichael for his help with quantitative real time PCR, A. Silva for generously providing access to his 2-photon microscope for some of these experiments, S. Kuhlman for her help with spike wave-form analysis, and E. Ruthazer for critical comments on earlier versions of this manuscript. This work was funded by grants from the National Eye Institute EY016052 and from the National Institute for Mental Health MH077972.

References

- Holtmaat A, Svoboda K. Experience-dependent structural synaptic plasticity in the mammalian brain. *Nat Rev Neurosci.* 2009; 10:647–658. [PubMed: 19693029]
- Zuo Y, Yang G, Kwon E, Gan WB. Long-term sensory deprivation prevents dendritic spine loss in primary somatosensory cortex. *Nature.* 2005; 436:261–265. [PubMed: 16015331]
- Hofer SB, Mrsic-Flogel TD, Bonhoeffer T, Hubener M. Experience leaves a lasting structural trace in cortical circuits. *Nature.* 2009; 457:313–317. [PubMed: 19005470]
- Trachtenberg JT, et al. Long-term in vivo imaging of experience-dependent synaptic plasticity in adult cortex. *Nature.* 2002; 420:788–794. [PubMed: 12490942]
- O'Connor DH, Peron SP, Huber D, Svoboda K. Neural activity in barrel cortex underlying vibrissa-based object localization in mice. *Neuron.* 2010; 67:1048–1061. [PubMed: 20869600]
- Dantzker JL, Callaway EM. Laminar sources of synaptic input to cortical inhibitory interneurons and pyramidal neurons. *Nat Neurosci.* 2000; 3:701–707. [PubMed: 10862703]
- Sohal VS, Zhang F, Yizhar O, Deisseroth K. Parvalbumin neurons and gamma rhythms enhance cortical circuit performance. *Nature.* 2009; 459:698–702. [PubMed: 19396159]
- Kasai H, Matsuzaki M, Noguchi J, Yasumatsu N, Nakahara H. Structure- stability-function relationships of dendritic spines. *Trends Neurosci.* 2003; 26:360–368. [PubMed: 12850432]
- Fiser J, Chiu C, Weliky M. Small modulation of ongoing cortical dynamics by sensory input during natural vision. *Nature.* 2004; 431:573–578. [PubMed: 15457262]
- Linden ML, Heynen AJ, Haslinger RH, Bear MF. Thalamic activity that drives visual cortical plasticity. *Nat Neurosci.* 2009; 12:390–392. [PubMed: 19252494]
- Komiyama T, et al. Learning-related fine-scale specificity imaged in motor cortex circuits of behaving mice. *Nature.* 2010; 464:1182–1186. [PubMed: 20376005]
- Thompson W. Synapse elimination in neonatal rat muscle is sensitive to pattern of muscle use. *Nature.* 1983; 302:614–616. [PubMed: 6835395]
- Zhang J, Ackman JB, Xu HP, Crair MC. Visual map development depends on the temporal pattern of binocular activity in mice. *Nat Neurosci.* 2011; 15:298–307. [PubMed: 22179110]
- Di Cristo G, et al. Subcellular domain-restricted GABAergic innervation in primary visual cortex in the absence of sensory and thalamic inputs. *Nat Neurosci.* 2004; 7:1184–1186. [PubMed: 15475951]
- Roberts TF, Tschida KA, Klein ME, Mooney R. Rapid spine stabilization and synaptic enhancement at the onset of behavioural learning. *Nature.* 2010; 463:948–952. [PubMed: 20164928]
- Arenkiel BR, et al. In vivo light-induced activation of neural circuitry in transgenic mice expressing channelrhodopsin-2. *Neuron.* 2007; 54:205–218. [PubMed: 17442243]
- Feng G, et al. Imaging neuronal subsets in transgenic mice expressing multiple spectral variants of GFP. *Neuron.* 2000; 28:41–51. [PubMed: 11086982]
- Dombeck DA, Khabbaz AN, Collman F, Adelman TL, Tank DW. Imaging large-scale neural activity with cellular resolution in awake, mobile mice. *Neuron.* 2007; 56:43–57. [PubMed: 17920014]

19. Kuhlman SJ, Tring E, Trachtenberg JT. Fast-spiking interneurons have an initial orientation bias that is lost with vision. *Nat Neurosci.* 2011; 14:1121–1123. [PubMed: 21750548]
20. Holtmaat A, et al. Long-term, high-resolution imaging in the mouse neocortex through a chronic cranial window. *Nat Protoc.* 2009; 4:1128–1144. [PubMed: 19617885]
21. Pologruto TA, Sabatini BL, Svoboda K. ScanImage: flexible software for operating laser scanning microscopes. *Biomed Eng Online.* 2003; 2:13. [PubMed: 12801419]
22. Holtmaat A, et al. Transient and persistent dendritic spines in the neocortex in vivo. *Neuron.* 2005; 45:279–291. [PubMed: 15664179]

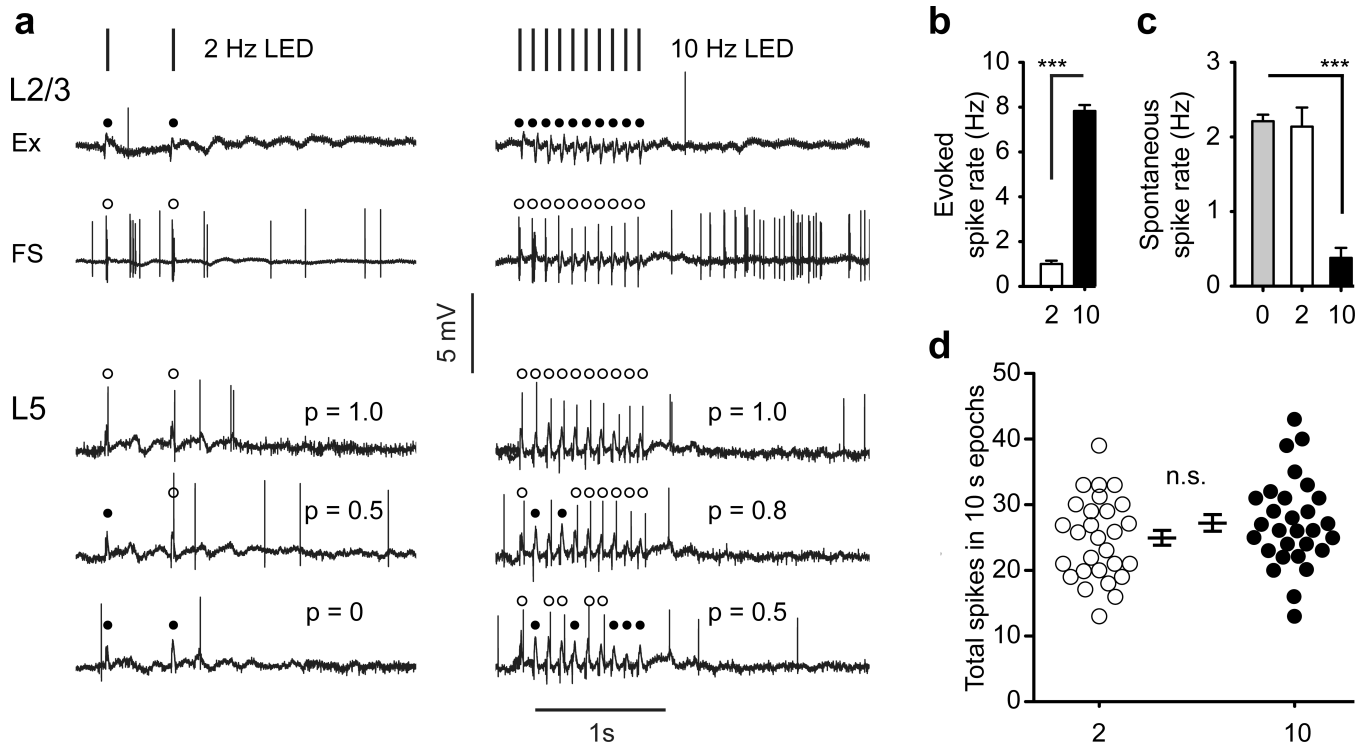


Figure 1. Chr2-mediated and spontaneous activity in awake mice

(a) Laminar and cell-type responses to 2 Hz (left) and 10 Hz (right) blue light trains. Example traces from a L2/3 excitatory neuron (Ex) and a L2/3 fast-spiking inhibitory neuron (FS) are shown. Filled circles indicate a failure to respond to a blue light pulse. Open circles identify successes. Note that Ex neurons fail to respond at either frequency while FS neurons respond to every light pulse. The lower three traces are from the same L5 excitatory neuron and show the variation in the evoked firing rate in this layer at the different stimulation frequencies. Probability of response is indicated for each trace with a ‘p=’. (b) Plot of evoked firing rate during 1-second trains of 2 Hz or 10 Hz light trains. (c) Plot of spontaneous activity during 1-second periods of normal wakefulness, and during 1-second trains of 2 Hz or 10 Hz light trains. (d) Scatter plots of total spiking measured over 10 second intervals in L5 neurons stimulated with the 2 Hz and 10 Hz light trains. 0=normal background activity, 2 = 2Hz stimulation, 10 = 10Hz stimulation. *** $P < 0.001$. Error bars are s.e.m.

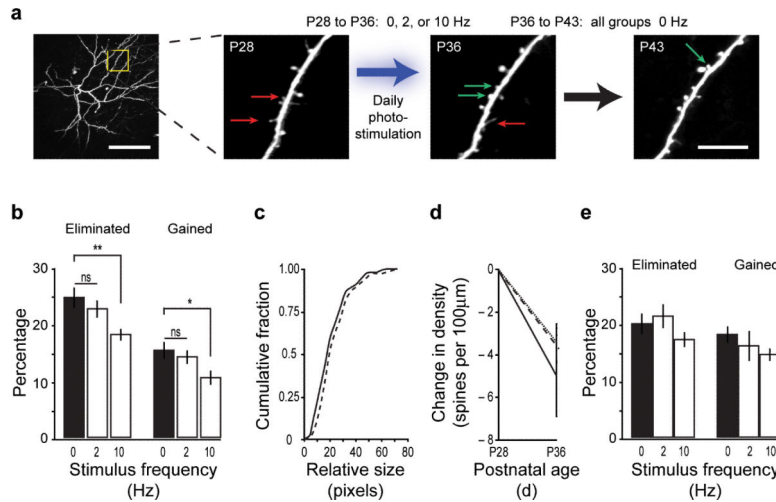


Figure 2. Spine stability is determined by the pattern of activity

(a, left) Low magnification image of the dendritic tree of a single L5 pyramidal neuron. The region highlighted in the yellow box is shown to the right. Scale bar is 100 μ m. (a, right) High magnification images of a dendritic region showing dendritic spines. Images were acquired at P28, P36, and P43. This example is from a mouse stimulated at 2 Hz from P28-P35, and unstimulated thereafter. Arrows show examples of gained (green) or lost (red) spines. Scale bar is 10 μ m. (b) Plot of percentage of spines gained or eliminated in each experimental group over a period of one week. * $P < 0.05$; ** $P < 0.01$ (c) Measure of relative spine size for eliminated spines in control (black line) and 10 Hz stimulated mice (dashed line). (d) Plot of change in spine density over one week in control (solid line), 2 Hz (dashed line), and 10 Hz (dotted line) groups. (e) Plot of percentage of spines gained or eliminated in each experimental group in the week following the cessation of optical stimulation. Error bars are s.e.m.